DNA damage tolerance in hematopoietic stem and progenitor cells in mice

Bas Pilzecker[a,1], Olimpia Alessandra Buoninfante[a,1], Paul van den Berk[a,1], Cesare Lancini[b], Ji-Ying Song[c], Elisabetta Citterio[b], and Heinz Jacobs[a,2]

[a]Division of Tumor Biology and Immunology, The Netherlands Cancer Institute, 1066 CX Amsterdam, The Netherlands; [b]Division of Molecular Genetics, The Netherlands Cancer Institute, 1066 CX Amsterdam, The Netherlands; and [c]Division of Experimental Animal Pathology, The Netherlands Cancer Institute, 1066 CX Amsterdam, The Netherlands

Edited by Tasuku Honjo, Graduate School of Medicine, Kyoto University, Kyoto, Japan, and approved July 5, 2017 (received for review April 20, 2017)

DNA damage tolerance (DDT) enables bypassing of DNA lesions during replication, thereby preventing fork stalling, replication stress, and secondary DNA damage related to fork stalling. Three modes of DDT have been documented: translesion synthesis (TLS), template switching (TS), and repriming. TLS and TS depend on site-specific PCNA K164 monoubiquitination and polyubiquitination, respectively. To investigate the role of DDT in maintaining hematopoietic stem cells (HSCs) and progenitors, we used *Pcna*$^{K164R/K164R}$ mice as a unique DDT-defective mouse model. Analysis of the composition of HSCs and HSC-derived multipotent progenitors (MPPs) revealed a significantly reduced number of HSCs, likely owing to increased differentiation of HSCs toward myeloid/erythroid-associated MPP2s. This skewing came at the expense of the number of lymphoid-primed MPP4s, which appeared to be compensated for by increased MPP4 proliferation. Furthermore, defective DDT decreased the numbers of MPP-derived common lymphoid progenitor (CLP), common myeloid progenitor (CMP), megakaryocyte-erythroid progenitor (MEP), and granulocyte-macrophage progenitor (GMP) cells, accompanied by increased cell cycle arrest in CMPs. The HSC and MPP phenotypes are reminiscent of premature aging and stressed hematopoiesis, and indeed progressed with age and were exacerbated on cisplatin exposure. Bone marrow transplantations revealed a strong cell intrinsic defect of DDT-deficient HSCs in reconstituting lethally irradiated mice and a strong competitive disadvantage when cotransplanted with wild-type HSCs. These findings indicate a critical role of DDT in maintaining HSCs and progenitor cells, and in preventing premature aging.

proliferating cell nuclear antigen K164 ubiquitination | DNA damage tolerance | hematopoietic stem and progenitor cells | translesion synthesis | template switching

Hematopoietic stem cells (HSCs) are able to maintain a steady population level over long periods through self-renewal. In addition, HSCs are pluripotent and can give rise to most specialized hematopoietic lineages (1, 2). Functionally distinct hematopoietic precursor subsets have been identified based on expression markers and functional transplantation analyses (3–5). These subsets are defined as long-term HSC (LT-HSC), short-term HSC (ST-HSC), multipotent progenitor 2–4 (MPP2, MPP3, and MPP4), common lymphoid progenitor (CLP), common myeloid progenitor (CMP), megakaryocyte-erythroid progenitor (MEP), and granulocyte-macrophage progenitor (GMP) (Table 1). The Lineage$^-$, Sca-1$^+$, cKit$^+$ (LSK) subset contains LT-HSC, ST-HSC, MPP2, MPP3, and MPP4. The hematopoietic stem and progenitor cell (HSPC) compartment comprises LT-HSC, ST-HSC, MPP2, and MPP3. The Lineage$^-$, cKit$^+$, Sca-1$^-$ (LKS$^-$) subset includes CMP, MEP, and GMP.

During aging, the HSC potential declines, and HSC differentiation is skewed toward the erythroid/myeloid-associated MPP2 lineage, seemingly at the expense of lymphoid-associated MPP4 and CLP (6). Consequently, lymphocyte production decreases and the functionality of the lymphoid system declines with aging. This age-related phenomenon of decreased lymphoid functionality, termed immunosenescence, is thought to be initiated in aging HSCs (7, 8).

Defects in DNA damage repair pathways progressively impair the fitness of HSCs and are linked to premature aging (7, 9–12). In addition, replicative stress has been implicated in HSC decline and aging (13). During S phase, DNA is copied by replicative polymerases epsilon and delta on the leading and lagging strands, respectively (14, 15). However, these replicative polymerases can be stalled by replication blocks, such as DNA lesions, G4 stacks, ribonucleotide misincorporation, and RNA/DNA hybrids that persist into or arise during S phase (16-18). To bypass such replication blocking lesions or structures and prevent secondary DNA damage due to prolonged fork stalling, three principle modes of DNA damage tolerance (DDT) are distinguished: translesion synthesis (TLS), template switching (TS), and repriming (19–23). PCNA K164-specific modifications are key to the ability to efficiently switch between a replicative mode and a damage-tolerant mode of DNA replication. In mammals, PCNA K164 can be sumoylated; however, sumoylation is not K164-specific (24). In contrast, DNA damage-induced monoubiquitination at lysine 164 of PCNA (PCNA-Ub) is site-specific and highly conserved.

PCNA-Ub facilitates efficient polymerase switching to a damage tolerant Y-family TLS polymerase that can accommodate non-Watson/Crick base pairs within their enlarged catalytic centers, enabling replication to continue across a lesion, albeit more error-prone. PCNA K164 polyubiquitination (PCNA-Ub^n) signals TS when the intact genetic information of the sister chromatid provides the template for an error-free bypass of the fork-stalling

Significance

The DNA damage response entails both DNA repair and DNA damage tolerance (DDT). DDT enables replicative bypass of fork-stalling DNA lesions and structures. Although DNA repair is known to be key in maintaining stem cells and tissue homeostasis, the contribution of DDT in stem cell maintenance remained to be defined. Using DDT-deficient *Pcna*$^{K164R/K164R}$ mice we here reveal a critical role of DDT in maintaining hematopoietic stem cells (HSCs). Defective DDT results in progressive impairment of HSCs, identifying DDT as a key player in preserving HSC fitness and prohibiting premature aging.

Author contributions: B.P., O.A.B., P.v.d.B., E.C., and H.J. designed research; B.P., O.A.B., P.v.d.B., C.L., and J.-Y.S. performed research; E.C. contributed new reagents/analytic tools; B.P., O.A.B., P.v.d.B., C.L., and J.-Y.S. analyzed data; and B.P., O.A.B., P.v.d.B., and H.J. wrote the paper.

The authors declare no conflict of interest.

This article is a PNAS Direct Submission.

Freely available online through the PNAS open access option.

[1]B.P., O.A.B., and P.v.d.B. contributed equally to this work.

[2]To whom correspondence should be addressed. Email: h.jacobs@nki.nl.

This article contains supporting information online at www.pnas.org/lookup/suppl/doi:10.1073/pnas.1706508114/-/DCSupplemental.

Table 1. Hematopoietic progenitor and HSC subsets and their markers

Subset	Subpopulations	Markers
LSK	HSPC, LT-HSC, ST-HSC, MPP2, MPP3, MPP4	Lineage$^-$, Sca-1$^+$, cKit$^+$
HSPC	LT-HSC, ST-HSC, MPP2, MPP3	Lineage$^-$, Sca-1$^+$, cKit$^+$, CD135$^-$
LT-HSC		Lineage$^-$, Sca-1$^+$, cKit$^+$, CD135$^-$, CD150$^+$, CD48$^-$
ST-HSC		Lineage$^-$, Sca-1$^+$, cKit$^+$, CD135$^-$, CD150$^-$, CD48$^-$
MPP2		Lineage$^-$, Sca-1$^+$, cKit$^+$, CD135$^-$. CD150$^+$, CD48$^+$
MPP3		Lineage$^-$, Sca-1$^+$, cKit$^+$, CD135$^-$, CD150$^-$, CD48$^+$
MPP4		Lineage$^-$, Sca-1$^+$, cKit$^+$, CD135$^+$
LKS-	CMP, GMP, MEP	Lineage$^-$, Sca-1$^-$, cKit$^+$
CMP		Lineage$^-$, Sca-1$^-$, cKit$^+$, CD34^{int}, CD16/32^{int}
GMP		Lineage$^-$, Sca-1$^-$, cKit$^+$, CD34$^+$, CD16/32$^+$
MEP		Lineage$^-$, Sca-1$^-$, cKit$^+$, CD34$^-$, CD16/32$^-$
CLP		Lineage$^-$, Sca-1^{int}, cKit^{int}, CD135$^+$, CD127$^+$

lesion. PCNA K164-independent mechanisms of TLS recruitment (e.g., the Y-family TLS polymerase REV1) can recruit other Y-family TLS polymerases to stalled forks (25-28). In *Saccharomyces cerevisiae*, a DDT-independent role of PCNA K164 modification has been suggested to play a minor role in lagging strand synthesis under unperturbed conditions (29), although that study could not exclude differential DDT activity on the leading vs. lagging strand in response to endogenous DNA damage and replication blocking lesions (19). In mammals, TLS is the predominant pathway, and PCNA-Ub–mediated TLS can be readily observed on DNA damage induction, whereas PCNA-Ub^n–mediated TS seems less frequent (30, 31). Recent research has highlighted the relevance of PCNA K164-dependent DDT in genome maintenance and its critical activity within the DNA damage response network (32–38); however, the overall relevance of these DDT pathways in the rapidly renewing hematopoietic system remained to be defined.

In this study, we investigated the role of DDT in HSC and progenitor cells. The contribution of DDT in the maintenance of HSCs was determined by analyzing the bone marrow (BM) of DDT-deficient *Pcna*$^{K164R/K164R}$ mice (34). Detailed analyses of the hematopoietic compartment of DDT-defective *Pcna*$^{K164R/K164R}$ mice

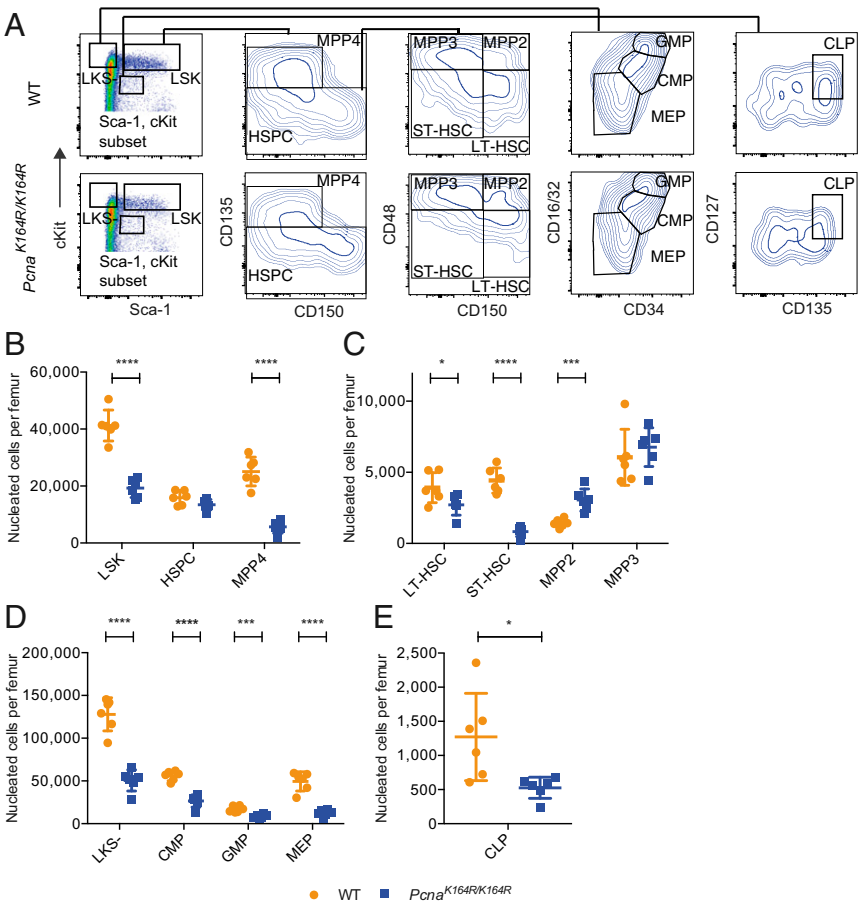

Fig. 1. PCNA K164R mutation leads to a HSC and progenitor defect. (*A*) Gating of hematopoietic precursor and HSC subsets in 2-mo-old WT and *Pcna*$^{K164R/K164R}$ mice. (*B–E*) Quantification of hematopoietic subsets in WT and *Pcna*$^{K164R/K164R}$ femora. Merged data from two experiments are shown, with a total of six mice per genotype. The *t* test was applied to calculate *P* values. *$P > 0.05$; ***$P > 0.001$; ****$P > 0.0001$.

revealed a critical contribution of DDT in determining the fitness of HSC and their progeny. A selective skewing of hematopoiesis toward the myeloid/erythroid-biased MPP2 in the LSK compartment indicated that defective DDT greatly accelerates aging of the hematopoietic compartment in $Pcna^{K164R/K164R}$ mice. These findings highlight the relevance and critical contribution of DDT analogous to DNA repair within the DNA damage response network, as well as the importance of DDT in safeguarding long-term tissue homeostasis.

Results

DDT Is Required to Maintain HSCs and Progenitor Cells. To investigate the relevance of DDT in maintaining HSCs and progenitors, we analyzed DDT-deficient mice with a $Pcna^{K164R/K164R}$ mutation. The distinct hematopoietic subsets were quantified using defined gating strategies and markers (3) (Table 1 and Fig. S1*A*). Following this strategy, the MPP1 subset is included in LT-HSCs.

In young adult mice (age 2 mo), the total number of nucleated cells per femur was comparable in WT and $Pcna^{K164R/K164R}$ mice; however, significant differences were found in various hematopoietic subsets. The LSK population in the BM was decreased by 2.1-fold, from 41×10^3 in WT compared with 19×10^3 cells per femur in $Pcna^{K164R/K164R}$ mice (Fig. 1 *A* and *B*). In the femora of $Pcna^{K164R/K164R}$ mice, LT-HSC was decreased by 1.4-fold, ST-HSC was decreased by 5.3-fold, and MPP4 was decreased by 4.4-fold. In contrast, the MPP2 subset was selectively increased by 2.1-fold in the $Pcna^{K164R/K164R}$ mice (Fig. 1 *B* and *C*).

The more differentiated LKS^- progenitor subset was also decreased, by 2.5-fold, in the $Pcna^{K164R/K164R}$ mice (Fig. 1*D* and Fig. S1*A*). Compared with WT, in $Pcna^{K164R/K164R}$ mice the CMP compartment decreased by 2.1-fold, GMP decreased by 1.9-fold, and MEP decreased by 4.0-fold. Furthermore, the CLP compartment decreased by 2.4-fold (Fig. 1*E*). MPP4 and CLP contribute primarily to lymphocytes (3). Given the decreased MPP4 and CLP in the $Pcna^{K164R/K164R}$ mice, we examined B and T lymphocyte development in these mice (Fig. S1 *B–D*). Using well-defined markers to trace lymphocyte differentiation (39), we found no major effects on B cell or T cell development. Similarly, splenic B cell and T cell populations remained largely unaffected, although B cells were slightly reduced.

To establish whether the defects in HSCs and other progenitor populations are due to increased DNA damage, we assayed the percentage of γH2AX-positive cells per subset (Figs. S2 *A–F* and S3). Because γH2AX increases during S/G2, we corrected for cell cycle status; i.e., percentages were calculated as γH2AX-positive cells in S/G2 of all cells in S/G2. γH2AX was slightly increased in all populations, although to a significant extent only in $Pcna^{K164R/K164R}$ LSK S/G2 cells, compared with WT.

In summary, the foregoing data indicate an important function of DDT in maintaining the HSC and progenitor populations in the BM. Furthermore, the decreases in ST-HSC and MPP4 combined with the increase of MPP2 is highly reminiscent of previously reported findings of hematopoietic regeneration and premature aging (3, 6).

DDT Deficiency Is Associated with Increased Proliferation and Cell Cycle Arrest in Distinct Hematopoietic Progenitor Subsets. Based on our findings of decreased numbers of cells in progenitor compartments and equal total BM cell numbers, we reasoned that the LSK and LKS^- progenitor compartments should increase proliferation to compensate for the decrease in progenitor cells. To examine

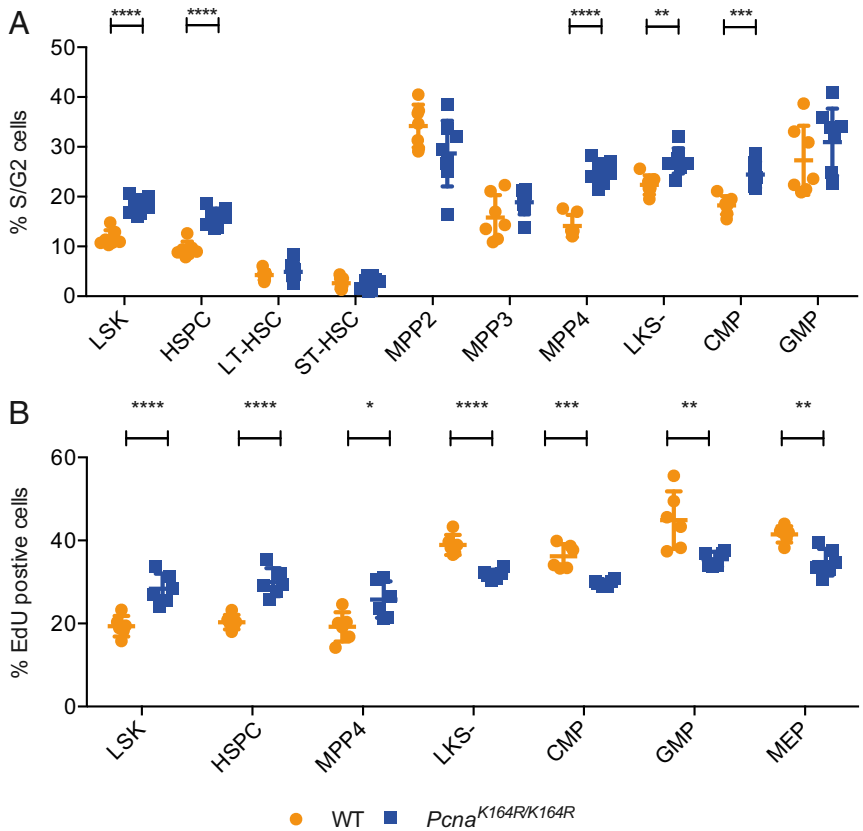

Fig. 2. Defective DDT leads to increased proliferation and cell cycle arrest in different hematopoietic subsets. (*A*) Percentage of S/G2 cells in WT and $Pcna^{K164R/K164R}$ in 2-mo-old mice. Combined data from two experiments are shown. (*B*) Percentage of EdU-positive cells in WT and $Pcna^{K164R/K164R}$ BM. Mice were treated with EdU for 24 h. Pooled data of two experiments are shown. The *t* test was used to calculate *P* values. *$P > 0.05$; **$P > 0.01$; ***$P > 0.001$; ****$P > 0.0001$.

whether the compromised early hematopoiesis in *Pcna*$^{K164R/K164R}$ mice leads to a compensatory proliferation or DDT deficiency-related cell cycle arrest at S/G2, we measured the chromatin content in HSCs and progenitor cells. In *Pcna*$^{K164R/K164R}$ BM cells, the percentage of cells in S/G2 was increased by 1.6-fold in the LSK population, by 1.6-fold in the HSPC population, and by 1.7-fold in the MPP4 population (Fig. 2*A* and Fig. S4). The increased percentage of S/G2 cells in the LSK and HSPC of *Pcna*$^{K164R/K164R}$ is most likely related to a selective increase in MPP2 cells per femur, which had a very high percentage of cells in S/G2. In contrast, within the HSPC population, no subset differed significantly in terms of percentage of cells in S/G2.

In the case of MPP4, the increase in S/G2 cells could be caused by increased proliferation or cell cycle arrest. To distinguish between these possibilities, we injected mice with the thymidine analog 5-ethynyl-2′-deoxyuridine (EdU) for 16 h. EdU incorporation into DNA enables quantification of actively proliferating cells. Following this approach, we observed that the frequency of EdU-positive cells in the MPP4 compartment was increased in *Pcna*$^{K164R/K164R}$ mice, supporting that idea that increased proliferation compensates for the lack of MPP4s (Fig. 2*B* and Fig. S5). The increased EdU incorporation in *Pcna*$^{K164R/K164R}$ LSK and HSPC compared with WT is likely relates to the presence of highly proliferative MPP2 precursors and their increased cell numbers in *Pcna*$^{K164R/K164R}$ mice.

In contrast to LSK, LKS$^-$ (1.2-fold) and CMP (1.3-fold) populations exhibited an increased S/G2 percentage and a reduced frequency of EdU-positive cells in *Pcna*$^{K164R/K164R}$ mice (Fig. 2 *A* and *B* and Fig. S5). These data suggest that the failure to tolerate endogenous DNA damage leads to an increased cell cycle arrest in the LKS$^-$ compartment of *Pcna*$^{K164R/K164R}$ mice.

In summary, these distinct alterations in the percentage of cells in S/G2 and EdU incorporation in LSK and LKS$^-$ subsets caused by the *Pcna*$^{K164R/K164R}$ mutation suggest that the BM subsets of these mice have differ in terms of endogenous replication impediments, sensitivity to DNA damage, and response to DNA damage signaling.

The Hematopoietic System of DDT-Deficient Mice Is Extraordinarily Sensitive to Cisplatin. Primary cell lines derived from *Pcna*$^{K164R/K164R}$ mice are highly sensitive to cisplatin (CsPt) (30, 35, 40). To quantify the sensitivity of *Pcna*$^{K164R/K164R}$ BM to interstrand and intrastrand cross-links, mice were injected i.v. with 0.8 mg/kg CsPt or mock-treated with PBS, and the BM was analyzed after 2 d. The dose used here was relatively low, because the maximal tolerable dose used in C57BL/6J mice is 6 mg/kg CsPt, which is 7.5-fold lower.

In WT mice, the total number of BM cells remained unaffected on low-dose CsPt treatment (Fig. 3 *A* and *B*). Pathological analysis of BM revealed that administration of low-dose CsPt at a concentration of 0.8 mg/kg did not visibly affect BM hematopoiesis in WT mice. Likewise, vehicle controls in both WT and *Pcna*$^{K164R/K174R}$ mutant mice showed no visible changes when mock-treated with PBS. In contrast, the *Pcna*$^{K164R/K164R}$ mutant mice showed massively disturbed myelopoiesis, erythropoiesis, and thrombopoiesis (Fig. 3*A* and Fig. S6). In particular, the erythropoietic population was greatly depleted.

Flow cytometry analysis of HSCs and progenitor cells revealed that in WT mice, only the CMP (1.3-fold decrease) and MEP populations (3-fold decrease) were affected on CsPt exposure, indicating that the myeloid/erythroid lineage is particularly sensitive to CsPt in WT mice (Fig. 3 and Fig. S6).

In line with the pathological analysis, counting total BM cells in *Pcna*$^{K164R/K164R}$ mice, CsPt treatment reduced the number of nucleated BM cells per femur from 18×10^6 in mock-treated mice to 10×10^6 in CsPt-treated mice, an 1.8-fold decrease (Fig. 3*B* and Fig. S6). Most remarkably, HSCs and progenitor cells were significantly affected. The LSK (57-fold), HSPC (41-fold), LT-HSC (52-fold), ST-HSC (335-fold), MPP2 (4-fold), MPP3 (32-fold),

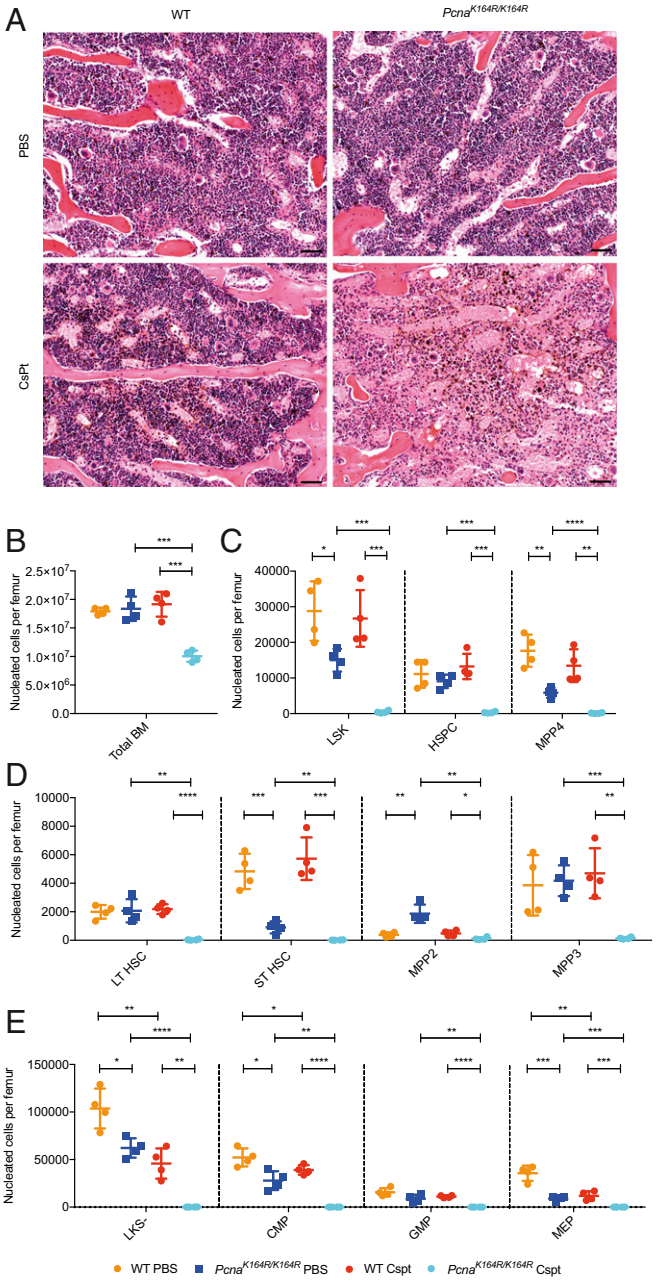

Fig. 3. The hematopoietic system strongly depends on DDT for tolerating cross-linking agents. (*A*) H&E-stained sternum of WT and *Pcna*$^{K164R/K164R}$ injected with PBS or CsPt. (Original magnification, 20×; scale bar, 50 μm.) (*B*–*E*) Number of nucleated cells per femur at 2 d after injection of 0.8 mg/kg CsPt or PBS. One representative experiment out of two experiments is shown. *$P > 0.05$; **$P > 0.01$; ***$P > 0.001$; ****$P > 0.0001$.

and MPP4 (102-fold) populations were severely diminished after CsPt treatment in *Pcna*$^{K164R/K164R}$ mice compared with CsPt-treated WT mice (Fig. 3 *C* and *D* and Fig. S6*A*). In the LKS$^-$ progenitors, the CMP (940-fold), GMP (219-fold), and MEP (1,755-fold) populations were all significantly reduced in *Pcna*$^{K164R/K164R}$ mice after treatment compared with the treated WT control mice (Fig. 3*E* and Fig. S6*A*). As expected, the subsets most strongly affected by CsPt were those with a higher S/G2 percentage, with the exception of ST-HSC and MPP2. ST-HSCs were decreased the most and MPP2 was decreased the least, suggesting that ST-HSCs can rapidly differentiate to MPP2 on stress to secure erythropoiesis.

In summary, the hematopoietic defect of DDT-deficient mice could be exacerbated by replication stress induced by CsPt. The PCNA K164 ubiquitination defect rendered HSC, MPP, and LKS$^-$-subsets highly sensitive to cross-linking agents. Not all hematopoietic subsets were equally impaired, however. In particular, ST-HSC, CMP, and MEP showed the largest fold change on CsPt exposure in both WT and *Pcna*$^{K164R/K164R}$ mice.

DDT Strongly Contributes to HSC Fitness. To determine the functionality of HSCs in *Pcna*$^{K164R/K164R}$ mice, we performed competitive BM transplantations. BM cells were transplanted by i.v. injection of a 1×10^6 1:1 mixture of Ly5.1 WT with Ly5.2 WT or *Pcna*$^{K164R/K164R}$ BM cells into irradiated Ly5.1 recipient mice. By applying the Ly5.1/Ly5.2 discrimination system, we determined the relative fitness of DDT-proficient and -deficient HSCs by measuring their contribution to the B lymphocytes, T lymphocytes, and granulocytes. In all three subsets, we observed that in the WT vs. WT setting, the contribution of Ly5.2 WT reached the expected plateau at 50–60% after 10 wk (Fig. 4 *A*–*C* and Fig. S7); however, in the *Pcna*$^{K164R/K164R}$ vs. WT setting, the contribution of Ly5.2 *Pcna*$^{K164R/K164R}$ was dramatically reduced. After 2 wk, there was a small contribution of Ly5.2 *Pcna*$^{K164R/K164R}$ cells to granulocytes and B cells, which might have arisen from differentiated progenitor cell populations. Their contribution further decreased to <5% after 5 wk and remained <5% for up to 20 wk.

In contrast, Ly5.2 *Pcna*$^{K164R/K164R}$ T cells start with a 50% contribution at 2 wk, likely derived from CLPs that populate the thymus (39). Similar to granulocytes and B cells, after 5 wk, the contribution of *Pcna*$^{K164R/K164R}$ also decreased to <5%.

At 20 wk after transplantation, we examined the BM and found that the population of HSCs containing LSK and more differentiated LKS$^-$ in the Ly5.2 *Pcna*$^{K164R/K164R}$ was almost absent, whereas WT Ly5.2 contributed 50%, as expected (Fig. 4*D*). These results indicate a severe defect in the transplantation capacity of *Pcna*$^{K164R/K164R}$ HSCs. These data also suggest that *Pcna*$^{K164R/K164R}$ HSCs are rapidly outcompeted by the WT HSCs or, alternatively, that *Pcna*$^{K164R/K164R}$ HSCs have difficulty in reaching the HSC niche.

To evaluate these hypotheses, we performed noncompetitive BM transplantations by i.v. injection of 2×10^6 Ly5.2 WT or *Pcna*$^{K164R/K164R}$ BM cells into irradiated syngeneic Ly5.1 recipient mice. After 2 wk and 4 wk, we assessed their transplantation capacity on the basis of Ly5.2 cells at different stages of hematopoiesis. In this noncompetitive BM transplantation assay, WT BM cells were much more effective in repopulating the depleted BM. After 2 wk, the femurs of WT reconstituted recipient mice contained 15×10^6 Ly5.2-positive cells, compared with only 6×10^6 cells in the femurs of *Pcna*$^{K164R/K164R}$ reconstituted recipient (Fig. 4*E*). This 2.5-fold reduction in reconstitution activity likely relates to intrinsic differences in the transplantation efficiency of *Pcna*$^{K164R/K164R}$ BM cells. This defect was even more pronounced

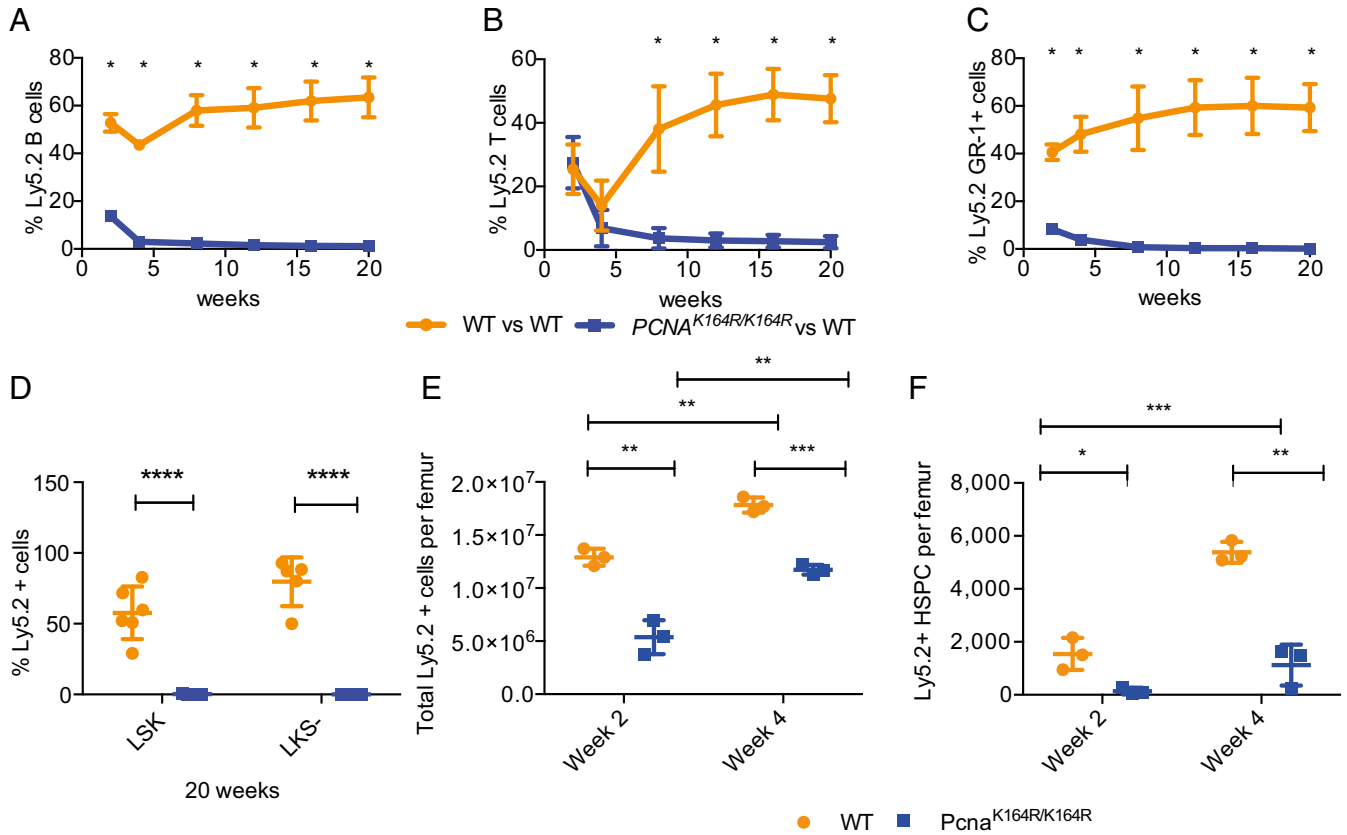

Fig. 4. PCNA K164R mutation leads to a HSC transplantation defect. (*A*–*C*) Competitive BM transplantation of WT or *Pcna*$^{K164R/K164R}$ Ly5.2 BM mixed with Ly5.1 BM transplanted into lethally irradiated Ly5.1 recipient mice. Contribution of Ly5.2 BM to the blood for B cells, T cells, and Gr-1$^+$ macrophages were measured for 20 wk. One representative experiment out of two experiments is shown. One million BM cells were transplanted in irradiated mice.*$P > 0.05$. (*D*) Percentage of Ly5.2-positive cells in the LSK and LKS$^-$ subset at 20 wk posttransplantation in WT and *Pcna*$^{K164R/K164R}$ mice, indicating the near absence of *Pcna*$^{K164R/K14R}$ HSC and precursor cells. One representative experiment out of two experiments is shown. (*E* and *F*) Short-term noncompetitive transplantation of WT or *Pcna*$^{K164R/K164R}$ BM. The total number of cells per femur (*E*) and number of HSC-containing HSPCs per femur (*F*) are shown. One million BM cells were transplanted in lethally irradiated mice. BM was isolated at 2 wk and 4 wk posttransplantation and analyzed. One representative experiment out of two experiments is shown. *$P > 0.05$; **$P > 0.01$; ***$P > 0.001$; ****$P > 0.0001$.

when analyzing HSCs containing LSK and HSPCs (Fig. 4*F* and Fig. S8 *A*–*F*). In addition, the LKS$^-$, CMP, GMP, and MEP progenitor population numbers were much lower after 2 wk in mice reconstituted with *Pcna*$^{K164R/K164R}$ BM. Even though the BM cellularity of *Pcna*$^{K164R/K164R}$ reconstituted recipients improved substantially after 4 wk, major differences remained in terms of defined BM precursor subsets. Of note, the observed differences at 2 wk after transplantation are not likely explained by preexisting differences in the initial subset composition of transplanted BM cells, because these differences greatly exceeded the preexisting differences.

In summary, these data indicate a severe intrinsic repopulation defect of *Pcna*$^{K164R/K164R}$ HSCs. This defect likely explains our observations in the competitive BM reconstitution assays.

DDT Deficiency Results in Premature Aging of the Early Hematopoietic Compartment. During aging, the number of MPP2 cells increases and the number of MPP4 cells progressively decreases in the BM (6). This suggests a priority for producing MPP2 at the expense of MPP4, because MPP2 cells are important precursors for the essential myeloid/erythrocyte lineage, and MPP4s are the precursors of the less important lymphoid lineage. In this way, oxygen supply is safeguarded. Interestingly, already after 2 mo, *Pcna*$^{K164R/K164R}$ mice showed an increased in MPP2 and a decrease in MPP4 cells. This phenotype caused by defective DDT is consistent with accelerated aging, presumably owing to increased replication stress. If this hypothesis is correct, then this phenotype would be expected to be further enhanced during aging. Thus, we compared the cellularity of the hematopoietic subsets of WT and *Pcna*$^{K164R/K164R}$ at age 9–10 mo (Fig. 5 *A*–*E*). Comparing 2-mo-old and 9- to 10-mo-old *Pcna*$^{K164R/K164R}$ and WT mice revealed further increases in fold changes in the ST-HSC, MPP4, and CLP subsets; however, MPP2 remained higher in the *Pcna*$^{K164R/K164R}$ mice throughout this period (Fig. S9). In contrast, in the LKS$^-$ subsets, aging did not increase the initial difference. This suggests that during stressed hematopoiesis, the maintenance of LKS$^-$ cells is a priority, because these cells contain the essential erythroid progenitors.

In summary, defective DDT leads to accelerated aging of the hematopoietic system, characterized by an increased selective skewing toward the MPP2 subset in LSK, primarily at the expense of the MPP4 subset.

Discussion

Although the role of DNA repair in HSC maintenance has been established, the contribution of DDT to HSC and progenitor maintenance has remained unclear. Here we report an elegant model for studying stressed hematopoiesis and demonstrate a critical cell-intrinsic role for DDT in maintaining adult HSCs and early hematopoiesis. *Pcna*$^{K164R/K164R}$ cells are defective in TLS and TS, leading to increased replication stress and sensitivity to fork-stalling DNA lesions. In 2-mo-old mice, the *Pcna*$^{K164R/K164R}$ mutation caused reduced cellularity of LSK, LT-HSC, ST-HSC, MPP4, LKS$^-$, CMP, GMP, MEP, and CLP subsets in the BM of mice. In contrast, the lack of PCNA K164-dependent

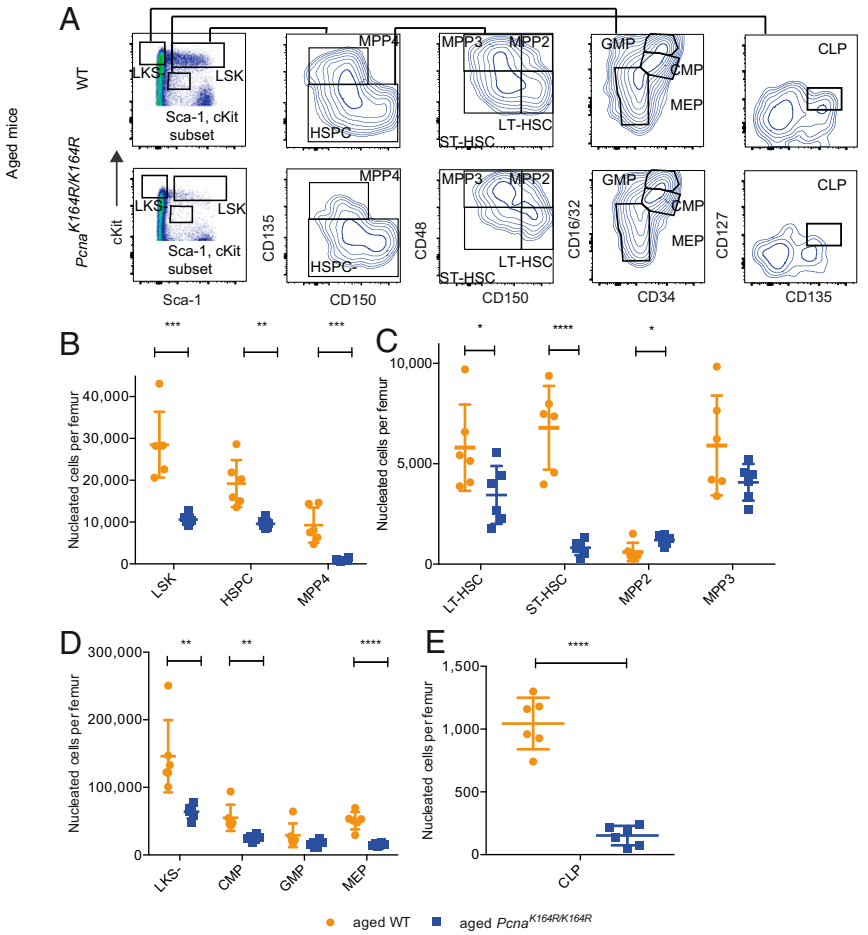

Fig. 5. Hematopoietic phenotype of DDT impaired mice is progressive with age. (*A*) FACS plots of 9- to 10-mo-old WT and *Pcna*$^{K164R/K164R}$ mice. (*B*–*E*) Number of nucleated cells per femur of different progenitors and HSC subsets in young (2 mo old) and aged (9–10 mo old) mice. *$P > 0.05$; **$P > 0.01$; ***$P > 0.001$; ****$P > 0.0001$.

DDT was associated with a selective increase in the myeloid/erythroid–associated MPP2 in $Pcna^{K164R/K164R}$ mice. This increase is likely due to increased stress-induced differentiation of HSCs, which reduces the number of HSCs, toward MPP2 at a cost of the number of MPP4 cells (3, 41, 42).

Our cell cycle and cell proliferation studies reveal an increased percentage of S/G2 cells and increased EdU incorporation in MPP4, suggestive of compensatory proliferation to counteract the strong loss of these lymphoid-primed progenitor cells. Because MPP4 mainly contributes to the lymphoid lineage, the increased proliferation could explain the unaffected B cell and T cell development in $Pcna^{K164R/K164R}$ mice. In contrast, LKS^{-} and CMP progenitors had an increased proportion of S/G2 cells combined with lower EdU incorporation in $Pcna^{K164R/K164R}$ mice, pointing to a cell cycle arrest caused by increased fork stalling and secondary DNA damage due to defective DDT.

To determine whether the BM defect of $Pcna^{K164R/K164R}$ mice could be enhanced by exogenous DNA damage, mice were exposed to CsPt. Although WT BM subsets were marginally affected, $Pcna^{K164R/K164R}$ HSC and progenitor subsets were almost depleted. This marked hypersensitivity to DNA damage in mice deficient for PCNA K164-dependent DDT further highlights the relevance of DDT in maintaining hematopoiesis and HSCs.

Aging is characterized by a selective skewing of hematopoiesis toward the myeloid/erythroid-associated MPP2 in the LSK subsets in aged mice (6). Therefore, the skewing toward MPP2 in the LSK compartment of $Pcna^{K164R/K164R}$ mice is likely related to accelerated aging induced by increased replication stress due to defective DDT. We hypothesize that stress-induced regeneration, like replication stress, of the hematopoietic system results in a shifted differentiation toward MPP2. This model is in line with previous reports documenting a shift toward MPP2 in the LSK compartment on stress-induced regeneration of the hematopoietic system (3). This skewing is further increased during aging. While the differentiation bias was already evident in 2-mo-old $Pcna^{K164R/K164R}$ mice, this bias increased further at age 9–10 mo. This finding supports the notion of accelerated aging in the $Pcna^{K164R/K164R}$ BM. Apparently, the capacity to tolerate DNA damage and prevent replication stress is critical to maintaining homeostasis in the BM compartment. The failure to tolerate DNA damage strongly accelerates aging of the BM compartment, indicating an important function of PCNA K164-dependent DDT in HSC maintenance. Defects in DNA repair pathways (9) and increased replication stress (13) have been identified as potent drivers of premature HSC aging, which is in line with our findings.

In our model of stressed hematopoiesis due to deficient DDT in $Pcna^{K164R/K164R}$ mice, HSCs shifted differentiation from mainly to MPP4 in WT to MPP2 in $Pcna^{K164R/K164R}$ (Fig. 6).

Of note, *Rad18*-deficient mice do not show a decrease of LSK cells (43). This likely is related to the existence of alternative E3 ligases targeting PCNA K164 (44, 45). Alternatively, an unknown PCNA K164 modification may play a role in maintaining HSCs and progenitor cells. An additional phenotype of $Pcna^{K164R/K164R}$ mice is infertility due to the complete absence of germ cells

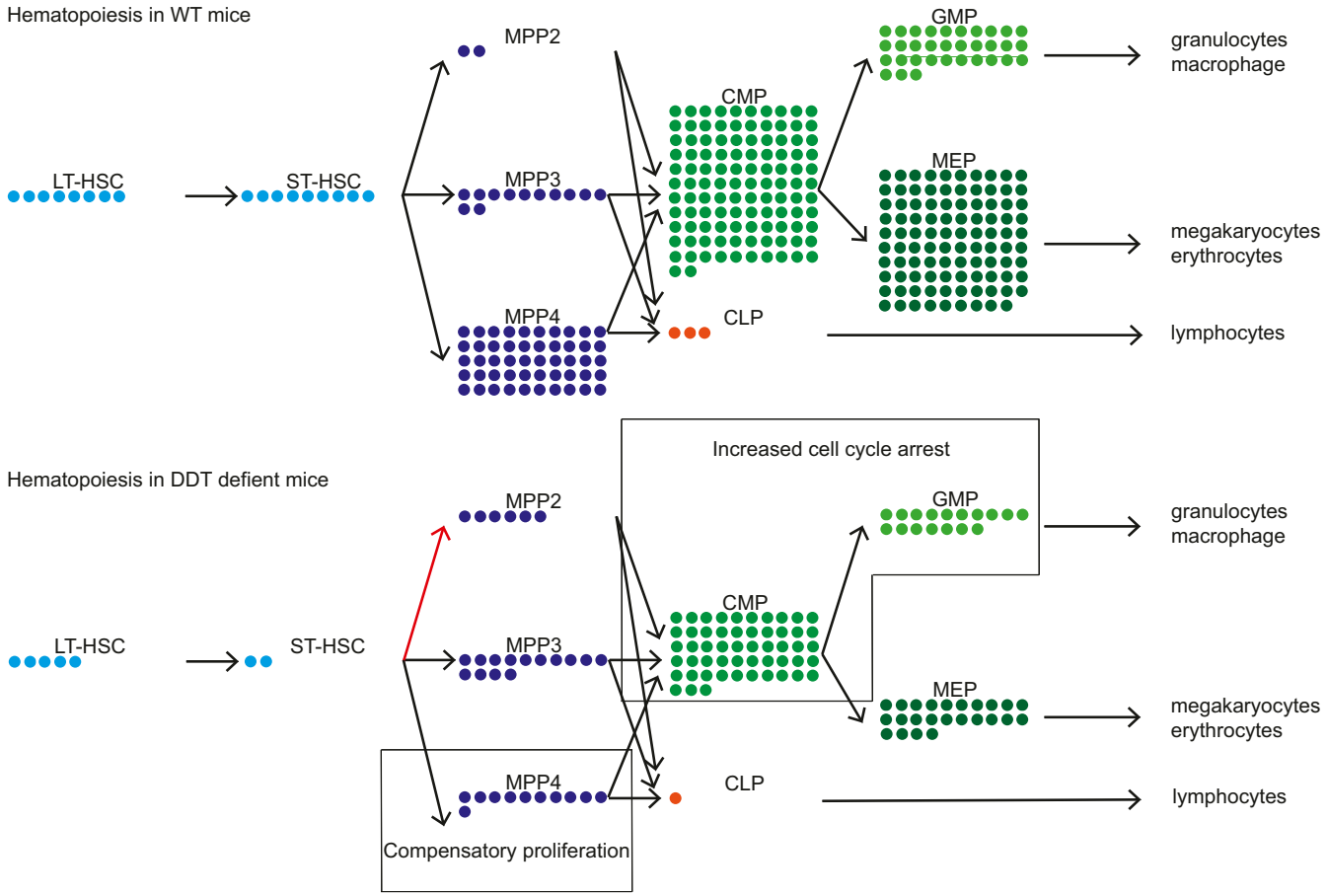

Fig. 6. Model for effect of DDT deficiency on HSC and early progenitors. Steady-state hematopoiesis in WT mice is indicated. In DDT-deficient $Pcna^{K164R/K164R}$ mice, replication stress-induced differentiation of HSC toward myeloid/erythroid-associated MPP2 in $Pcna^{K164R/K164R}$ is indicated by a red arrow. Compensatory proliferation for MPP4 is specified, as is cell cycle arrest in CMP and GMP subsets. Arrows indicate the direction of differentiation. The blue dots indicate LSK subsets, and the green dots indicate LKS^{-} subsets. Each dot represents 500 nucleated cells per femur.

(34). The infertility, the BM phenotype, and the sensitivity to cross-linking agents are shared phenotypes with Fanconi anemia (FA) mouse models (46–48). Future research should examine the contribution of PCNA K164-dependent DDT in the FA pathway.

The FA pathway is involved in the repair of interstrand cross-links (49, 50). DDT pathways, on the other hand, likely tolerate a myriad of replication blocks. These replication blocks may include base damages such as deamination, methylation, and oxidation; intrastrand and interstrand cross-links induced by endogenous and exogenous genotoxins; G4 stacks; RNA-DNA hybrids; and ribonucleotide misincorporation (16-18, 51, 52). Consequently, DDT-impaired HSCs are likely to be sensitized to this complex spectrum of lesions. For survival, PCNA K164-deficient DDT HSCs are assumed to depend on alternative DDT pathways, such as REV1-dependent DDT. Given the impact of a DDT defect on HSCs, it is likely that other stem cells, especially those in highly proliferative compartments, are sensitive as well. Further research is needed to examine the sensitivity of other tissue stem cells and the relevance of DDT for tissue homeostasis.

In conclusion, this study reports the relevance of DDT in preventing premature aging in the hematopoietic compartment and safeguarding HSC functionality. These data highlight DDT as important arm of the DNA damage response network.

Methods

Mice and Breeding. The *Pcna*$^{K164R/K164R}$ knock-in mouse model has been described previously (34). All mice were kept on C57BL/J6 background under specific pathogen-free conditions. *Pcna*^{K164R} mice were maintained heterozygous. All experiments were approved by the Animal Experimental Commission of the Netherlands Cancer Institute and performed in accordance with Dutch and European guidelines.

Antibodies. Antibody specifications are listed in Table S1.

Flow Cytometry.

Hematopoietic precursor subset analysis. Mice were killed at the indicated age (2 mo or 9–10 mo), and BM from femora was flushed out using a 21-gauge syringe with cold PBEA buffer (1× PBS 0.5% BSA, 2 mM EDTA, and 0.02% sodium azide). The samples were kept on ice. We used 5×10^6 cells per staining. BM cells were first stained with a biotinylated lineage + antibody mix for 30 min and then washed twice in PBEA buffer. For quantifying stem cells and MPP populations, cKit-APC, Sca-1-PerCp/Cy5.5, CD48-FITC, CD135-PE, CD150-PE/Cy7, and streptavidin-APC/Cy7 were used. For quantifying LKS$^-$ progenitor populations, cKit-APC, CD34-FITC, CD16/32-PE/Cy7, streptavidin-APC/Cy7, and Sca-1-Pacific Blue were used. To quantify CLPs, cKit-APC, CD127-PerCp/Cy5.5, CD135-PE, streptavidin-APC/Cy7, and Sca-1-Pacific Blue were used. Cells were washed twice with PBEA and then resuspended in 400 μL of PBEA. For stem cells and MPP, DAPI was used as life/dead staining, whereas for LKS$^-$ and CLP, propidium iodide (PI) was used. All measurements were performed with a BD LSRFortessa cell analyzer (BD Biosciences). Analyses were performed using FlowJo version 10.0.8r1.

Cell cycle analysis of BM populations. Cell surface staining was performed as described above. Samples were incubated in Cytofix/Cytoperm (BD Biosciences) for 15 min. Cells were washed using Permwash and harvested in PBEA containing 10 μg/mL DAPI. Analyses were performed using FlowJo version 10.0.8r1.

Assessing γH2AX levels of BM populations. Cell surface staining was performed as described above. BM cells were first labeled with biotinylated Lin+ antibody mix. Subsequently, LSK populations were stained with CD135-PE, SCA-1-PerCp/Cy5.5, cKit-APC, and streptavidin-APC/Cy7. Progenitor populations were stained with SCA-1-PerCpCy5.5, CD16/32-PE/Cy7, cKit-APC, and streptavidin-APC/Cy7.

Cells were fixed and permeabilized using Cytofix/Cytoperm (BD Biosciences), then stained with γH2AX antibody for 30 min at room temperature. Anti-mouse IgG-AF488 was used for the secondary staining. DAPI (10 μg/mL) was used for chromatin labeling. A nonspecific IgG isotype control served as a negative control. Analyses were performed using FlowJo version 10.0.8r1.

B and T development. The lymphocyte composition and precursor subsets in thymus and bone marrow were analyzed as described previously (19).

In vivo EdU incorporation assay. Here 200 μL of 10 mM EdU in PBS was injected i.p. After 16 h, BM was isolated as described above. The Click-iT Plus EdU Flow Cytometry Kit AF488 (Thermo Fisher Scientific) protocol was followed. BM was stained using biotinylated Lineage+ antibody mix, cKit-APC, Sca-1-PerCp/Cy5.5, CD135-PE, CD150-PE/Cy7, and streptavidin-APC/Cy7, followed by Alexa Fluor 488 picolyl azide staining. A non–EdU-treated mouse served as a negative control. Analyses were performed using FlowJo version 10.0.8r1.

Competitive BM Reconstitution. BM was isolated from three Ly5.2 2-mo-old WT mice and three 2-mo-old Ly5.2 *PCNA*^{K164RK164R} mice and mixed 1:1 with the BM isolated from one Ly5.1 WT mouse. Thereafter, 1×10^6 Ly5.1/Ly5.2 mixed BM cells were transplanted into lethally irradiated (two doses of 5.5 Gy, separated by a 3-h interval) Ly5.1 recipient mice. Blood (50 μL) was obtained after 2, 4, 8, 12, 16, and 20 wk. The contribution in the blood of Ly5.1 and Ly5.2 cells was assessed using Ly5.1-PE and Ly5.2-PE/Cy7 antibodies. Cells were also stained with Gr1-APC/Cy7, CD3-FITC, CD19-APC, and CD11b-PerCp/Cy5.5 for subset analysis. DAPI was used for life/death staining. At 20 wk posttransplantation, the mice were killed, and the BM was isolated for analysis, as described above using SCA-1-PerCp/Cy5.5, cKit-APC, streptavidin APC/Cy7, Ly5.1-PE, and Ly5.2-PE-Cy7. Irradiated mice were treated with Enrobactin for the first 4 wk after irradiation. Analyses were performed using FlowJo version 10.0.8r1.

Noncompetitive BM Transplantation. The BM of Ly5.2 WT and *Pcna*$^{K164R/K164R}$ mice was isolated. Recipient Ly5.1 mice were lethally irradiated (two doses of 5.5 Gy, separated by a 3-h interval) and transplanted with 1×10^6 WT or *Pcna*$^{K164R/K164R}$ BM cells. At 2 wk and 4 wk posttransplantation, BM and blood were isolated to assess the contribution of the transplanted BM, as described above. Analyses were performed using FlowJo version 10.0.8r1.

In Vivo CsPt Sensitivity Assay. Mice were injected i.v. with 0.8 mg/kg cisplatin or PBS. After 2 d, the BM was isolated and analyzed as described above.

Calculations and Statistics. We determined the number of viable cells per subset by DAPI or PI staining and based on the ratio of subset of interest and viable population times the number of cells per femur. The number of cells per femur was standardized to 20×10^6 when no difference in total BM numbers was found between WT and *Pcna*$^{K164R/K164R}$. The *t* tests were performed using GraphPad Prism version 6.0. In the figures, $*P > 0.05$; $**P > 0.01$; $***P > 0.001$; $****P > 0.0001$.

ACKNOWLEDGMENTS. We thank H. te Riele and N. Wit for comments on the manuscript, A. Pfauth, F. van Diepen, and M. van Baalen for cell sorting and assistance during flow cytometry, and the animal caretakers of the NKI-AVL for biotechnical assistance. This project was made possible by generous support from the Dutch Cancer Foundation (Grants KWF NKI-2012-5243 and KWF NKI-2016-10032, to H.J.).

1. Orford KW, Scadden DT (2008) Deconstructing stem cell self-renewal: Genetic insights into cell-cycle regulation. *Nat Rev Genet* 9:115–128.
2. Morrison SJ, Uchida N, Weissman IL (1995) The biology of hematopoietic stem cells. *Annu Rev Cell Dev Biol* 11:35–71.
3. Pietras EM, et al. (2015) Functionally distinct subsets of lineage-biased multipotent progenitors control blood production in normal and regenerative conditions. *Cell Stem Cell* 17:35–46.
4. Cabezas-Wallscheid N, et al. (2014) Identification of regulatory networks in HSCs and their immediate progeny via integrated proteome, transcriptome, and DNA methylome analysis. *Cell Stem Cell* 15:507–522.
5. Wilson A, et al. (2008) Hematopoietic stem cells reversibly switch from dormancy to self-renewal during homeostasis and repair. *Cell* 135:1118–1129.
6. Young K, et al. (2016) Progressive alterations in multipotent hematopoietic progenitors underlie lymphoid cell loss in aging. *J Exp Med* 213:2259–2267.
7. Geiger H, de Haan G, Florian MC (2013) The ageing haematopoietic stem cell compartment. *Nat Rev Immunol* 13:376–389.
8. Le Saux S, Weyand CM, Goronzy JJ (2012) Mechanisms of immunosenescence: Lessons from models of accelerated immune aging. *Ann N Y Acad Sci* 1247:69–82.
9. Rossi DJ, et al. (2007) Deficiencies in DNA damage repair limit the function of haematopoietic stem cells with age. *Nature* 447:725–729.
10. Parmar K, et al. (2010) Hematopoietic stem cell defects in mice with deficiency of Fancd2 or Usp1. *Stem Cells* 28:1186–1195.
11. Prasher JM, et al. (2005) Reduced hematopoietic reserves in DNA interstrand crosslink repair-deficient Ercc1$^{-/-}$ mice. *EMBO J* 24:861–871.
12. Rossi DJ, Jamieson CH, Weissman IL (2008) Stems cells and the pathways to aging and cancer. *Cell* 132:681–696.
13. Flach J, et al. (2014) Replication stress is a potent driver of functional decline in ageing haematopoietic stem cells. *Nature* 512:198–202.

14. Nick McElhinny SA, Gordenin DA, Stith CM, Burgers PM, Kunkel TA (2008) Division of labor at the eukaryotic replication fork. *Mol Cell* 30:137–144.
15. Miyabe I, Kunkel TA, Carr AM (2011) The major roles of DNA polymerases epsilon and delta at the eukaryotic replication fork are evolutionarily conserved. *PLoS Genet* 7:e1002407.
16. Sarkies P, Reams C, Simpson LJ, Sale JE (2010) Epigenetic instability due to defective replication of structured DNA. *Mol Cell* 40:703–713.
17. Helmrich A, Ballarino M, Nudler E, Tora L (2013) Transcription-replication encounters, consequences and genomic instability. *Nat Struct Mol Biol* 20:412–418.
18. Nick McElhinny SA, et al. (2010) Genome instability due to ribonucleotide incorporation into DNA. *Nat Chem Biol* 6:774–781.
19. Pilzecker B, et al. (2016) PrimPol prevents APOBEC/AID family-mediated DNA mutagenesis. *Nucleic Acids Res* 44:4734–4744.
20. Bianchi J, et al. (2013) PrimPol bypasses UV photoproducts during eukaryotic chromosomal DNA replication. *Mol Cell* 52:566–573.
21. García-Gómez S, et al. (2013) PrimPol, an archaic primase/polymerase operating in human cells. *Mol Cell* 52:541–553.
22. Sale JE, Lehmann AR, Woodgate R (2012) Y-family DNA polymerases and their role in tolerance of cellular DNA damage. *Nat Rev Mol Cell Biol* 13:141–152.
23. Moldovan GL, Pfander B, Jentsch S (2007) PCNA, the maestro of the replication fork. *Cell* 129:665–679.
24. Gali H, et al. (2012) Role of SUMO modification of human PCNA at stalled replication fork. *Nucleic Acids Res* 40:6049–6059.
25. Guo C, et al. (2003) Mouse Rev1 protein interacts with multiple DNA polymerases involved in translesion DNA synthesis. *EMBO J* 22:6621–6630.
26. Ohashi E, et al. (2004) Interaction of hREV1 with three human Y-family DNA polymerases. *Genes Cells* 9:523–531.
27. Tissier A, et al. (2004) Co-localization in replication foci and interaction of human Y-family members, DNA polymerase pol eta and REVl protein. *DNA Repair (Amst)* 3: 1503–1514.
28. Acharya N, Haracska L, Prakash S, Prakash L (2007) Complex formation of yeast Rev1 with DNA polymerase eta. *Mol Cell Biol* 27:8401–8408.
29. Becker JR, et al. (2015) Genetic interactions implicating postreplicative repair in Okazaki fragment processing. *PLoS Genet* 11:e1005659.
30. Wit N, et al. (2015) Roles of PCNA ubiquitination and TLS polymerases κ and η in the bypass of methyl methanesulfonate-induced DNA damage. *Nucleic Acids Res* 43: 282–294.
31. Krijger PH, et al. (2011) HLTF and SHPRH are not essential for PCNA polyubiquitination, survival and somatic hypermutation: Existence of an alternative E3 ligase. *DNA Repair (Amst)* 10:438–444.
32. Stelter P, Ulrich HD (2003) Control of spontaneous and damage-induced mutagenesis by SUMO and ubiquitin conjugation. *Nature* 425:188–191.
33. Hoege C, Pfander B, Moldovan GL, Pyrowolakis G, Jentsch S (2002) RAD6-dependent DNA repair is linked to modification of PCNA by ubiquitin and SUMO. *Nature* 419: 135–141.
34. Langerak P, Nygren AO, Krijger PH, van den Berk PC, Jacobs H (2007) A/T mutagenesis in hypermutated immunoglobulin genes strongly depends on PCNAK164 modification. *J Exp Med* 204:1989–1998.
35. Hendel A, et al. (2011) PCNA ubiquitination is important, but not essential for translesion DNA synthesis in mammalian cells. *PLoS Genet* 7:e1002262.
36. Edmunds CE, Simpson LJ, Sale JE (2008) PCNA ubiquitination and REV1 define temporally distinct mechanisms for controlling translesion synthesis in the avian cell line DT40. *Mol Cell* 30:519–529.
37. Bienko M, et al. (2005) Ubiquitin-binding domains in Y-family polymerases regulate translesion synthesis. *Science* 310:1821–1824.
38. Kannouche PL, Wing J, Lehmann AR (2004) Interaction of human DNA polymerase η with monoubiquitinated PCNA: A possible mechanism for the polymerase switch in response to DNA damage. *Mol Cell* 14:491–500.
39. Rodewald HR, Fehling HJ (1998) Molecular and cellular events in early thymocyte development. *Adv Immunol* 69:1–112.
40. Krijger PH, et al. (2011) PCNA ubiquitination-independent activation of polymerase η during somatic hypermutation and DNA damage tolerance. *DNA Repair (Amst)* 10: 1051–1059.
41. Santos MA, et al. (2014) DNA-damage-induced differentiation of leukaemic cells as an anti-cancer barrier. *Nature* 514:107–111.
42. Wang J, et al. (2016) Per2 induction limits lymphoid-biased haematopoietic stem cells and lymphopoiesis in the context of DNA damage and ageing. *Nat Cell Biol* 18: 480–490.
43. Yang Y, et al. (2016) Rad18 confers hematopoietic progenitor cell DNA damage tolerance independently of the Fanconi Anemia pathway in vivo. *Nucleic Acids Res* 44: 4174–4188.
44. Simpson LJ, et al. (2006) RAD18-independent ubiquitination of proliferating-cell nuclear antigen in the avian cell line DT40. *EMBO Rep* 7:927–932.
45. Terai K, Abbas T, Jazaeri AA, Dutta A (2010) CRL4(Cdt2) E3 ubiquitin ligase monoubiquitinates PCNA to promote translesion DNA synthesis. *Mol Cell* 37:143–149.
46. Bakker ST, de Winter JP, te Riele H (2013) Learning from a paradox: Recent insights into Fanconi anaemia through studying mouse models. *Dis Model Mech* 6:40–47.
47. Parmar K, D'Andrea A, Niedernhofer LJ (2009) Mouse models of Fanconi anemia. *Mutat Res* 668:133–140.
48. Garaycoechea JI, Patel KJ (2014) Why does the bone marrow fail in Fanconi anemia? *Blood* 123:26–34.
49. Kottemann MC, Smogorzewska A (2013) Fanconi anaemia and the repair of Watson and Crick DNA crosslinks. *Nature* 493:356–363.
50. Deans AJ, West SC (2011) DNA interstrand crosslink repair and cancer. *Nat Rev Cancer* 11:467–480.
51. Lindahl T, Barnes DE (2000) Repair of endogenous DNA damage. *Cold Spring Harb Symp Quant Biol* 65:127–133.
52. Ciccia A, Elledge SJ (2010) The DNA damage response: Making it safe to play with knives. *Mol Cell* 40:179–204.